

Article

# Thermodynamic Behaviour of Mixed Films of an Unsaturated and a Saturated Polar Lipid. (Oleic Acid-Stearic Acid and POPC-DPPC)

Juan Torrent-Burgués 

Department of Chemical Engineering, Universitat Politècnica de Catalunya, C/Colom 1, E-08222 Terrassa, Barcelona, Spain; juan.torrent@upc.edu

Received: 30 January 2018; Accepted: 25 April 2018; Published: 27 April 2018



**Abstract:** Mixed fatty acids or mixed phospholipids systems with saturated-unsaturated hydrocarbon chains are of biological interest. In this work, the monolayers of oleic acid-stearic acid (OA-SA) and palmitoyl-oleoylphosphatidylcholine-dipalmitoylphosphatidylcholine (POPC-DPPC) have been studied. From the surface pressure-area isotherms, elastic modulus values and virial equation coefficients can be obtained. Thermodynamic treatment also yields excess ( $G^E$ ) and mixing ( $\Delta G_{mix}$ ) free energies. Results indicate positive  $G^E$  values, that is, molecular interactions in the mixed films are less favourable, due to the presence of unsaturation; however, the mixture is slightly favourable due to the entropic factor that affords positive  $\Delta G_{mix}$  values. For the OA-SA system, a high SA content and surface pressure facilitate the phase separation, even though a certain miscibility between both components still remains. For the POPC-DPPC system, the most favourable mixing conditions occur for  $X_{POPC} \approx 0.4$ . For these mixed systems, the values of the elastic modulus are more similar to those of more fluid components (OA or POPC); analysis of the virial coefficients shows that the  $b_1$  virial coefficient values lie between those of the individual components and are higher than values suitable for an ideal mixing.

**Keywords:** mixed films; fatty acids; phosphatidylcholines;  $\pi$ -A isotherms; virial state equation

## 1. Introduction

Fatty acids and phospholipids have been widely studied with the Langmuir technique, because they are amphiphilic compounds, ideal for forming ordered and compact monolayers, and for their biological interest in systems as biomembranes and tear films. Bibliographic references to previous studies can be found in [1–3]. Articles on single component fatty acids or related amphiphiles published in the last years are those of [4–16], and articles on single component phospholipids are those of [17–22].

As mixtures of fatty acids or phospholipids are found in biological systems, the study of such mixtures is more interesting. One of the main aspects of these mixtures is the miscibility and phase separation. Recent articles on mixed fatty acids systems are those of [23–32]. Furthermore, since fatty acids or phospholipids usually present unsaturations in the hydrocarbon chains, the study of mixtures of saturated and unsaturated compounds is of interest. Recent articles on fatty acid systems with mixed saturated-unsaturated hydrocarbon chains are those of [33,34], and on phospholipids systems with mixed saturated-unsaturated hydrocarbon chains are those of [35–44]. The main achievements reported in these works will be commented in the discussion section, in connection with the results of the present work. Briefly, an important point considered in these works is the miscibility and phase separation of Langmuir films composed of a mixture of a lipid with a saturated chain and a lipid with an unsaturated chain. Ocko et al. [33] found that stearic acid and elaidic acid were poorly miscible in monolayers at all surface pressures, and phase separation was

always observed. Seoane et al. [34] studied the miscibility of cholesterol with several fatty acids, and found immiscibility between stearic acid and cholesterol and partial miscibility between unsaturated fatty acids and cholesterol. Wydro et al. [44] found that DPPG mix non-ideally with DPPE, DSPE and DOPE. They suggest that in the DPPG-DOPE system, and due to the presence of the double bonds in the acyl chains of DOPE molecule, the distance between DPPG and DOPE molecules is greater; this weakens the strength of molecular interactions. Their results indicate that DPPG mix more favourably with PE possessing saturated acyl chains as compared to DOPE, and also suggests the existence of a phase separation for DPPG-DOPE monolayers. Dynarowicz-Latka et al. [37] found immiscibility between DPPC and erucylphosphocholine, a synthetic one-chained-PC with a double bond, at high surface pressures, but miscibility at low surface pressures. Domenech et al. [35] observed miscibility between POPC and POPE, and using the virial equation of state, analysed the interactions between both. In other works [43], the influence of cholesterol in mixed films has been studied; the results indicate an important effect of cholesterol in the monolayer structure.

Despite the wide literature in the field, no recent articles in the study in deep of stearic acid and oleic acid mixed films or DPPC-POPC mixed films, which are of biological relevance [45], have been reported. Mixed films of a lipid with a saturated acyl chain and a lipid with an unsaturated acyl chain were selected, since unsaturation seems to have a great influence in the miscibility of both lipids. In this work, these mixed films have been studied using the surface pressure-area,  $\pi$ - $A$ , isotherms. The thermodynamic behaviour of the mixed films has been analysed through the excess area, the elastic modulus, and the virial state equation, the latter not being very usual in the treatment of monolayer films.

The elastic modulus,  $C_s^{-1}$ , was determined according to Equation (1) [46–49]

$$C_s^{-1} = -A \left( \frac{d\pi}{dA} \right)_T \quad (1)$$

In this study, the virial state equation, Equation (2), has been applied, where  $b_0$ ,  $b_1$  and  $b_2$  are the virial coefficients. The virial state equation is useful and allows, through the virial coefficients, for an examination of molecular interactions [35,50]; in this case, it will be applied to the effect of an unsaturation in the acyl chain over the molecular interactions. The value of  $b_0$  is attributed to the aggregation state of the film-forming molecules, and the value of  $b_1$  provides information about the exclusion volumes and the interaction between the molecules in the film.

$$\pi A / (kT) = b_0 + b_1 \cdot \pi + b_2 \cdot \pi^2 \quad (2)$$

The following treatment can be applied to the virial coefficients in a mixture [35], where  $X$  refers to the molar fraction, the subscripts 1 and 2 refer to the individual components, the subscripts  $m$  and 12 refer to the mixture, and the superscripts  $id$  and  $E$  referring to an ideal behaviour and to an excess magnitude, respectively:

$$b_{1)m} = b_{1)1} \cdot X_1^2 + b_{1)2} \cdot X_2^2 + 2b_{1)12} \cdot X_1 \cdot X_2 \quad (3)$$

$$b_{1)m}^{id} = b_{1)1} \cdot X_1 + b_{1)2} \cdot X_2 \quad (4)$$

$$b_1^E = b_{1)m} - b_{1)m}^{id} \quad (5)$$

The thermodynamic behaviour of the system can also be analysed from Equations (6) to (9), where  $A^E$  is the excess area,  $A_{12}$  is the mean area per molecule for the mixture,  $A_1$  and  $A_2$  are the area per molecule and  $X_1$  and  $X_2$  are the molar fraction, for the individual components. On the other hand,  $N_A$  is Avogadro's number,  $R$  is the gas constant and  $T$  is the absolute temperature.  $G^E$  refers to the excess free energy,  $\Delta G_{mix}$  and  $\Delta G_{id}$  refer to the Gibbs energy of mixing and its ideal value, respectively.

$$A^E = A_{12} - (X_1 A_1 + X_2 A_2) \quad (6)$$

$$G^E = N_A \int_0^\pi A^E d\pi \quad (7)$$

$$\Delta G_{mix} = \Delta G_{id} + G^E \quad (8)$$

$$\Delta G_{id} = RT(X_1 \cdot \ln X_1 + X_2 \cdot \ln X_2) \quad (9)$$

Introducing the virial equation, Equation (2), in the former equations, then Equation (10) is obtained for the excess free energy,  $G^E$ , which can be calculated from the values of the virial coefficients according to Equations (11)–(13). This treatment is rarely seen in bibliography, and offers an alternative way to calculate excess free energy values.

$$G^E = RT [B_0 \cdot \ln \pi + B_1 \cdot (\pi - 1) + B_2 / 2 \cdot (\pi^2 - 1)] \quad (10)$$

$$B_0 = b_{0m} - X_1 \cdot b_{01} - X_2 \cdot b_{02} \quad (11)$$

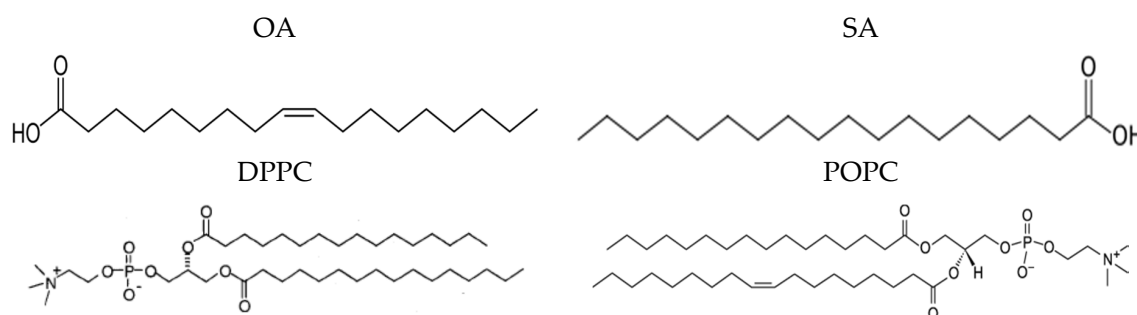
$$B_1 = b_{1m} - X_1 \cdot b_{11} - X_2 \cdot b_{12} \quad (12)$$

$$B_2 = b_{2m} - X_1 \cdot b_{21} - X_2 \cdot b_{22} \quad (13)$$

## 2. Materials and Methods

### 2.1. Materials

Stearic acid (SA) was provided by Sigma-Aldrich and oleic acid (OA) by Fluka. Dipalmitoylphosphatidylcholine (DPPC) and palmitoyloleoylphosphatidylcholine (POPC) were purchased from Avanti Polar Lipids. See Scheme 1 for chemical structures.  $\text{KH}_2\text{PO}_4$ , NaCl and analytical grade chloroform from Sigma-Aldrich (Saint Louis, MO, USA) were used in solution preparation. Water was ultrapure MilliQ<sup>®</sup> (18.2 M $\Omega$ ·cm).



**Scheme 1.** Structural formula of the studied compounds: SA, OA, DPPC and POPC.

### 2.2. Techniques

Langmuir monolayer formation was carried on a trough (Nima Technology, Cambridge, UK) model 1232D1D2 equipped with two movable barriers. The surface pressure was measured using paper Whatman 1, held by a Wilhelmy balance connected to a microelectronic system registering the surface pressure ( $\pi$ ). The subphase used in these experiments was MilliQ<sup>®</sup> quality water. Prior to the subphase addition, the trough was cleaned twice with chloroform and once with MilliQ<sup>®</sup> quality water. Residual impurities were cleaned from the air | liquid interface by surface suctioning. The good baseline in the surface pressure-area,  $\pi$ -A, isotherms confirms the interface's cleanliness. Solutions of the lipids were prepared using chloroform; 100  $\mu\text{L}$  were spread at the air | liquid interface, using a high precision Hamilton microsyringe. Individual solutions were prepared at a concentration of 0.5 mg/mL for the fatty acids and 1 mg/mL for the phospholipids, and from them the mixtures were obtained. The barrier closing rate was fixed at 50  $\text{cm}^2 \cdot \text{min}^{-1}$  for isotherm registration (4.7  $\text{\AA}^2 \cdot \text{molecule}^{-1} \cdot \text{min}^{-1}$  for fatty acids and 6.1  $\text{\AA}^2 \cdot \text{molecule}^{-1} \cdot \text{min}^{-1}$  for phospholipids), but no noticeable influence of the compression

rates between 25 and 50  $\text{cm}^2 \cdot \text{min}^{-1}$  was observed on the isotherm shape. Isotherm recording was carried out by adding the solution, drop by drop, to the subphase, and waiting 15 min for a perfect spreading and solvent evaporation. Experiments were conducted at  $22 \pm 1$  °C and repeated a minimum of three times for reproducibility control.

### 3. Results and Discussion

#### 3.1. SA-OA Mixture

The  $\pi$ -A isotherms for the mixed films of SA and OA, together to those of the individual components, are shown in Figure 1; in Figure 2 the values of mean area are plotted vs. the molar fraction at several surface pressures.

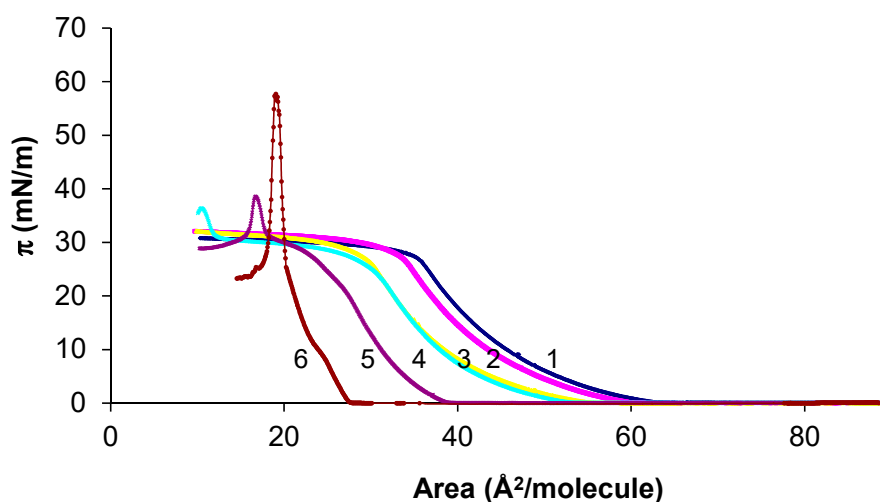


**Figure 1.**  $\pi$ -A isotherms for mixtures of OA-SA. 1, (blue) OA; 2, (magenta)  $X_{\text{OA}} = 0.816$ ; 3, (yellow)  $X_{\text{OA}} = 0.625$ ; 4, (cyan)  $X_{\text{OA}} = 0.425$ ; 5, (violet)  $X_{\text{OA}} = 0.217$ ; 6, (brown) SA. Area represents the mean area per molecule.

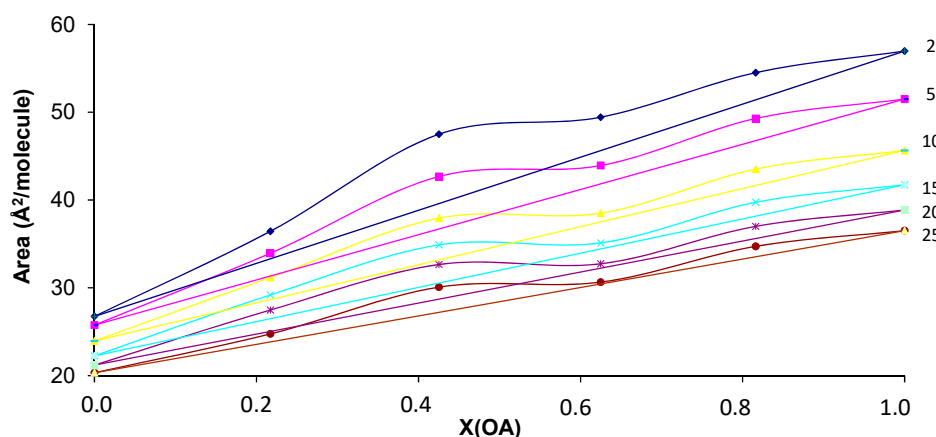


**Figure 2.** Area vs. composition for mixtures OA-SA, at different surface pressures: (blue) 2, (magenta) 5, (yellow) 10, (cyan) 15, (violet) 20, (brown) 25 mN/m. The straight lines correspond to the ideal behaviour.

Mixed monolayers show a first collapse that practically coincides with that of OA ( $\pi = 30 \text{ mN} \cdot \text{m}^{-1}$ ), and when the proportion of SA increases, a second collapse is observed (isotherms 4 and 5 in Figure 1) which does not reach the value observed for SA ( $\pi = 58 \text{ mN} \cdot \text{m}^{-1}$ ). This is an indication that at high surfaces pressures, OA forms a separated phase from SA which collapses at surface pressure

( $30 \text{ mN}\cdot\text{m}^{-1}$ ); meanwhile, the collapse of the SA phase is influenced by the presence of OA. Thus, the OA molecules strongly distort on the compactness of the SA molecules and hamper the formation of a more rigid film.

A study of the mean area per molecule (Figure 2) shows positive deviations from the straight line; these deviations are more pronounced at low surface pressures and when the OA content is  $X_{\text{OA}} = 0.425$ . At high surface pressures and with all compositions except for the OA content of  $X_{\text{OA}} = 0.425$ , the mean area approaches a straight line. Positive deviations indicate mixing but with unfavourable interactions with respect to pure components. Null deviations indicate an ideal mixing or phase separation. As two collapses can be observed in the isotherms when the SA is in high proportion, this indicates that a phase separation has occurred. As experimental points are not on the straight line, this means that partial miscibility still exists, that is, a partial segregation of one component occurs but the rest of this component remains on the mixed film.

Figure 3 presents the variation of the elastic modulus, Equation (1), along the isotherm compression for the different mixed films of SA and OA. According to the reported criteria, that is  $C_s^{-1}$ :  $<100 \text{ mN}\cdot\text{m}^{-1}$  for LE state,  $100\text{--}250 \text{ mN}\cdot\text{m}^{-1}$  for LC state,  $>250 \text{ mN}\cdot\text{m}^{-1}$  for S state [47,51], OA shows an LE state, meanwhile SA shows an LE state below  $9 \text{ mN}\cdot\text{m}^{-1}$ , an LC state between  $9\text{--}24 \text{ mN}\cdot\text{m}^{-1}$  and an S state up to  $24 \text{ mN}\cdot\text{m}^{-1}$ . On the other hand, mixed films show an LE state, and for those with higher OA content, the compressibility behaviour is similar to that of pure OA; however, when the SA content is high, an LC state appears at higher surface pressures.

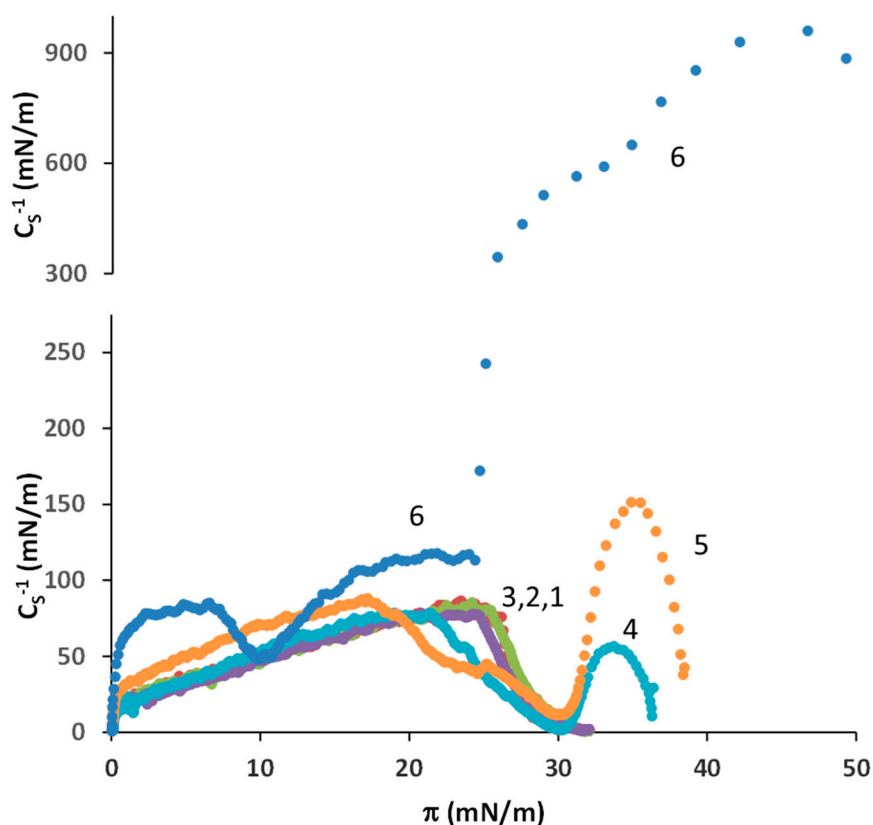


**Figure 3.** Elastic modulus for mixtures of OA-SA. 1, (brown) OA; 2, (green)  $X_{\text{OA}} = 0.816$ ; 3, (violet)  $X_{\text{OA}} = 0.625$ ; 4, (cyan)  $X_{\text{OA}} = 0.425$ ; 5, (orange)  $X_{\text{OA}} = 0.217$ ; 6, (blue) SA.

It is also seen that when the SA content increases, the surface pressure at the inflection point in the isotherm, or at the first maximum point in the elastic modulus plot, decreases. In contrast, the second maximum point in the elastic modulus plot increases with more SA content. These results also

point to a partial mixing at low surface pressures but a segregation at high surface pressures, especially at high SA content.

To gain a deeper understanding at the molecular level, the surface pressure-area isotherms of SA-OA mixtures were further analysed using the equation of state. For this study, the virial state equation, Equation (2), was applied. Figure 4 shows the plots of  $(\pi A/kT)$  vs.  $\pi$  for the several studied compositions, which can be adjusted with a polynomial of  $2n$  degree. The values of the virial coefficients are tabulated in Table 1. The values of  $b_{1|12}$  and  $b_1^E$ , obtained from Equations (3)–(5), are tabulated in Table 2.

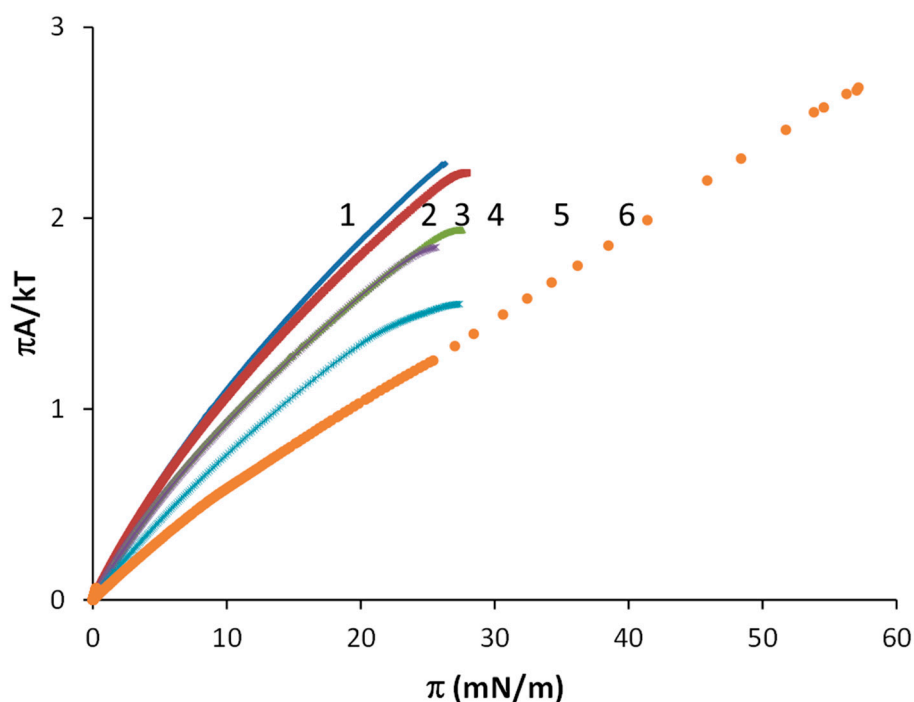


**Figure 4.** Plots of  $(\pi A/kT)$  vs.  $\pi$  for the mixtures of OA-SA. 1, (blue) OA; 2, (red)  $X_{OA} = 0.816$ ; 3, (green)  $X_{OA} = 0.625$ ; 4, (violet)  $X_{OA} = 0.425$ ; 5, (cyan)  $X_{OA} = 0.217$ ; 6, (orange) SA.

**Table 1.** Virial coefficients (see Equation (2)) for mixtures of OA and SA.

Virial Coefficient	OA	OA-SA $X_{OA} = 0.816$	OA-SA $X_{OA} = 0.625$	OA-SA $X_{OA} = 0.425$	OA-SA $X_{OA} = 0.217$	SA
$b_0$	0.0055	0.0050	0.0046	0.0048	0.0007	−0.0021
$b_1$	0.1255	0.1208	0.1080	0.1064	0.0883	0.0566
$b_2$	−0.0015	−0.0015	−0.0014	−0.0013	−0.0011	−0.00018
$R^2$	0.9994	0.9994	0.9994	0.9997	0.9999	0.9974

**Table 2.** Virial coefficient  $b_1$  (see Equations (3)–(5)) for mixtures of OA and SA.

$X_{OA}$	$b_{1 m}$	$b_{1 12}$	$b_1^E$
0	0.0566		0
0.217	0.0883	0.1403	0.0167
0.425	0.1064	0.1330	0.0205
0.625	0.1080	0.1088	0.0083
0.816	0.1208	0.1176	0.0080
1	0.1255		0

Results for  $b_1$  coefficients (see Table 2) indicate a gradual decrease from the OA pure component to the SA one. A similar fact occurs for the  $b_0$  coefficient. The higher value for  $b_1$  of OA is due to the higher repulsive interactions between molecules in this fatty acid, relative to the SA. The higher value for  $b_0$  of OA is due to a lesser degree of aggregation in this fatty acid with respect to the SA. The values of  $b_{1,m}$  are in between those of the SA and OA, but higher than those of the ideal behaviour, that is, the  $b_1^E$  values are positive. This indicates more repulsive interactions in the mixed films between SA and OA molecules with respect to the separate components. The values of  $b_{1,12}$  are positive and higher than the mean value  $(b_{1,1} + b_{1,2})/2 = 0.09105$ , which also indicates more repulsion in the mixed film between molecules. The higher values of  $b_{1,12}$  occur when the content of OA is low, being higher than the value of  $b_1$  of pure OA. This fact can be attributed to the fact that OA breaks the compactness of SA, which results in an increase of the  $b_1$  coefficient (much more repulsion in respect to pure components).

As positive deviations are higher for low OA content, low  $X_{OA}$ , this means that OA places partially in between SA, destabilizing the compactness of SA. When there is a low SA content, it can better mix with the fluid phase of OA, the interactions are less unfavourable and the positive deviations are lower. Thus, the domain formation or phase separation could be more notable for low  $X_{OA}$ , that is, for high SA content.

Introducing the values of virial coefficients in Equations (6)–(9) and (10)–(13), values of  $G^E$  and  $\Delta G_{mix}$  were calculated and are reported in Table 3. It is seen that  $G^E$  exhibits positive values which were considered as small deviations from zero excess free energy; the values of  $\Delta G_{mix}$  are slightly negative. These values are in agreement with the previous comments about the mixing of the components in the film, that is, the interaction between components is not favoured but the entropic factor (see Equation (9)) leads to energetically favourable mixing, even with slightly negative values of  $\Delta G_{mix}$ . Mixing is less favoured especially at higher SA contents and higher surface pressures.

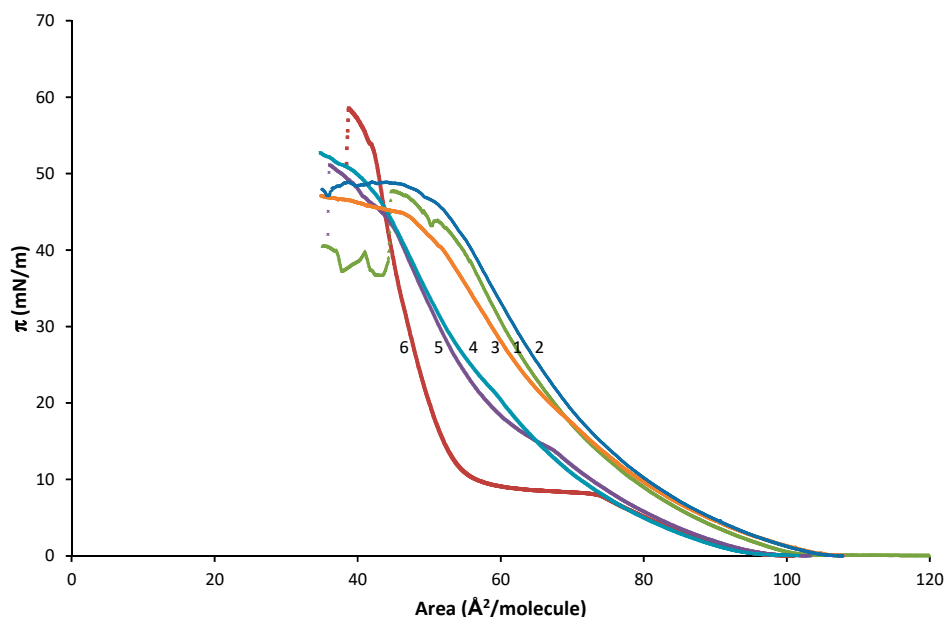
**Table 3.** Values of excess free energy and mixing energy at different compositions and surface pressures for OA-SA mixed films.

$\pi$ (mN/m)	$X_{OA}$	0.816	0.625	0.425	0.217
5	$G^E$ (J/mol)	75	78	199	150
	$\Delta G_{mix}$ (J/mol)	−1096	−1545	−1473	−1133
15	$G^E$ (J/mol)	213	191	575	409
	$\Delta G_{mix}$ (J/mol)	−958	−1432	−1097	−874
25	$G^E$ (J/mol)	291	204	809	510
	$\Delta G_{mix}$ (J/mol)	−880	−1419	−863	−773

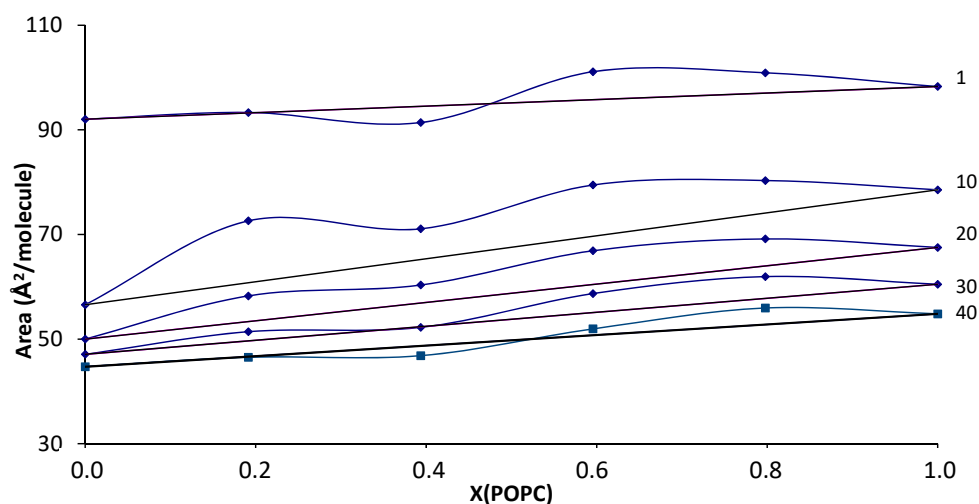
### 3.2. DPPC-POPC Mixture

Figure 5 shows the  $\pi$ -A isotherms of mixed films of DPPC and POPC, together with those of the individual components. It was observed that the phase change of DPPC at  $\pi = 8$  mN/m (the first inflection point) are influenced by the presence of POPC, as well as the collapse pressure, indicating that DPPC and POPC are partially miscible. The inflection point is clearly visible at the lowest content of POPC and the surface pressure at which this point occurs increases with the POPC content.

Figure 6 shows the mean area per molecule vs. the POPC molar fraction, at several  $\pi$ . Positive deviations respect to the ideal case (straight line) were generally observed, but at low and high  $\pi$ , the mixed film with  $X_{POPC} = 0.394$  presents negative deviations which indicate less repulsive interactions or more attractive interactions (favourable interactions in respect to the individual components). In both cases, deviations from the straight line indicate a certain degree of miscibility. This fact will be commented upon later.



**Figure 5.**  $\pi$ -A isotherms for mixtures of POPC-DPPC. 1, (green) POPC; 2, (blue)  $X_{\text{POPC}} = 0.798$ ; 3, (orange)  $X_{\text{POPC}} = 0.596$ ; 4, (cyan)  $X_{\text{POPC}} = 0.394$ ; 5, (violet)  $X_{\text{POPC}} = 0.191$ ; 6, (brown) DPPC. Area represents the mean area per molecule.



**Figure 6.** Area vs. composition in mixtures POPC-DPPC, at the surface pressures of 1, 10, 20, 30 and 40 mN/m.

Figure 7 shows the elastic modulus of DPPC, POPC and DPPC-POPC mixed films, obtained from the isotherms of Figure 5 using Equation (1). DPPC presents a phase change from LE to LC at  $\pi$  around 8 mN/m, and POPC only presents LE state. The fact that DPPC can present the LC state in the monolayer is related to the chain melting temperature of 41 °C for DPPC, against that of  $-2$  °C for POPC [52]. Thus, at the temperature of the present work, POPC is always in the LE state; however, DPPC can change from the LE to the LC state when compressing. The DPPC-POPC studied mixed films only presents the LE state, with an inflection at high DPPC contents, and the inflexion surface pressure increasing when the DPPC content decreases. This fact clearly confirms that POPC mixes with DPPC, and thus that POPC molecules hamper a more compaction of DPPC molecules and the phase change to a LC state.

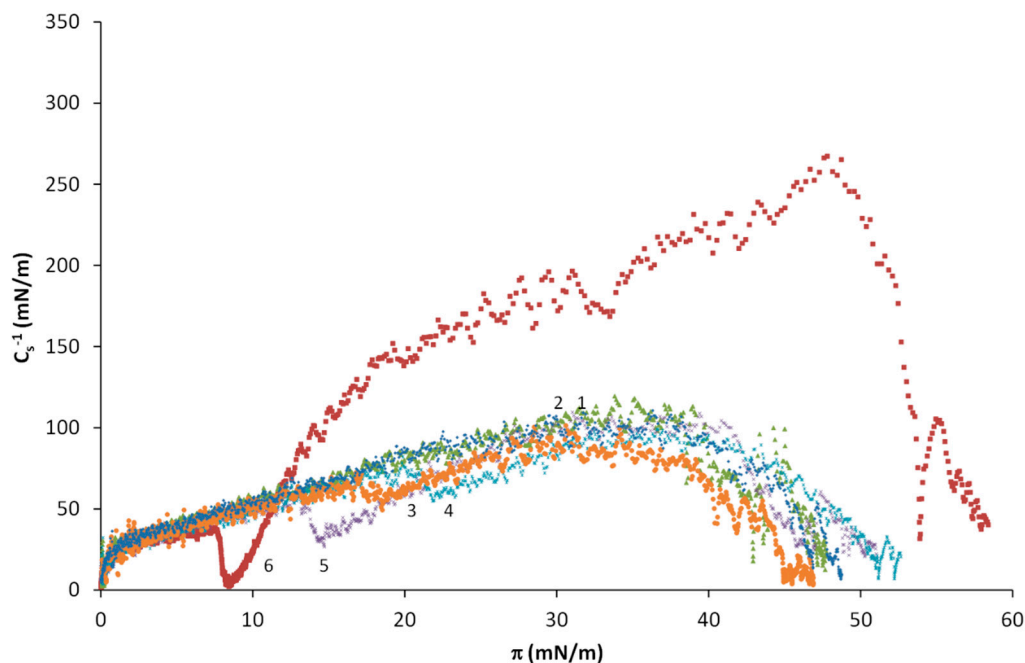


**Figure 7.** Elastic modulus for mixtures of POPC-DPPC. 1, (green) POPC; 2, (blue)  $X_{\text{POPC}} = 0.798$ ; 3, (orange)  $X_{\text{POPC}} = 0.596$ ; 4, (cyan)  $X_{\text{POPC}} = 0.394$ ; 5, (violet)  $X_{\text{POPC}} = 0.191$ ; 6, (brown) DPPC.

An analysis of the isotherms using the virial state equation has been done.

The plot of  $\pi A / (kT)$  vs.  $\pi$  (Figure 8) can be fitted with a polynomial of  $2n$  degree (see Equation (2)), and the treatment reported in Equations (3)–(5) is applied to them. The values of the obtained virial coefficients are tabulated in Table 4 and the values of  $b_{1|12}$  and  $b_1^E$  in Table 5.

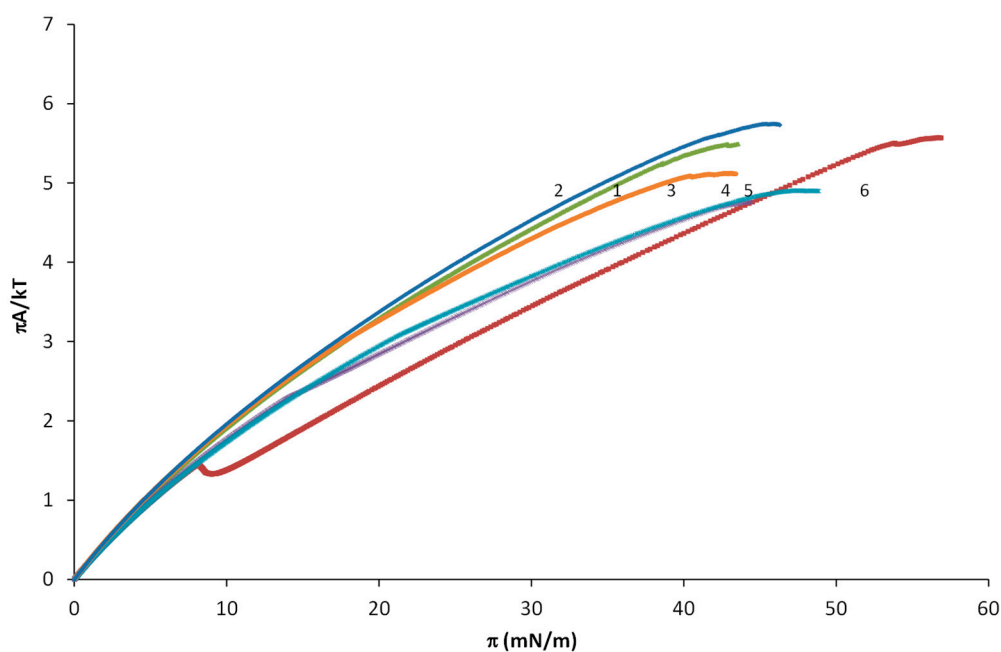


**Figure 8.** Plots of  $(\pi A / kT)$  vs.  $\pi$  for the mixtures of POPC-DPPC. 1, (green) POPC; 2, (blue)  $X_{\text{POPC}} = 0.798$ ; 3, (orange)  $X_{\text{POPC}} = 0.596$ ; 4, (cyan)  $X_{\text{POPC}} = 0.394$ ; 5, (violet)  $X_{\text{POPC}} = 0.191$ ; 6, (brown) DPPC.

**Table 4.** Virial coefficients (see Equation (2)) for mixtures of POPC and DPPC.

Virial Coefficient	POPC	POPC:DPPC $X_{\text{POPC}} = 0.798$	POPC:DPPC $X_{\text{POPC}} = 0.596$	POPC:DPPC $X_{\text{POPC}} = 0.394$	POPC:DPPC $X_{\text{POPC}} = 0.191$	DPPC
$b_0$	0.0319	0.0856	0.0923	0.0832	0.0978	0.1930
$b_1$	0.2002	0.1991	0.1984	0.1744	0.1736	0.1333
$b_2$	-0.0017	-0.0016	-0.0019	-0.0016	-0.0016	-0.00068
$R^2$	0.9994	0.9995	0.9992	0.9989	0.9970	0.9916

**Table 5.** Virial coefficient  $b_1$  (see Equations (3)–(5)) for mixtures of POPC and DPPC.

$X_{\text{POPC}}$	$b_{1,m}$	$b_{1,12}$	$b_1^E$
0	0.1333		0
0.191	0.1736	0.256	0.0275
0.394	0.1744	0.198	0.0147
0.596	0.1984	0.219	0.0252
0.798	0.1991	0.205	0.0124
1	0.2002		0

It is shown in Table 4 that the  $b_1$  values increase with the POPC content. This indicates more repulsive interactions for POPC, and that the presence of POPC in the DPPC matrix also increases the repulsive interactions between molecules with respect to DPPC molecules. The value of  $b_0$  for POPC is lower than that of DPPC, indicating more aggregation in POPC than in DPPC (even POPC has an unsaturation in the hydrocarbon chain, the oleoyl chain is larger. Another explanation could be in the phase change of DPPC that makes the polynomial fit more problematic). The values of  $b_{1,m}$  are in between those of the DPPC and POPC, but higher than those of the ideal behaviour, that is, the  $b_1^E$  values are positive. This indicates more repulsive interactions in the mixed film between DPPC and POPC molecules with respect to the separate components. The values of  $b_{1,12}$  are positive and higher than the mean value  $(b_{1,1} + b_{1,2})/2 = 0.1667$ , which also indicates more repulsion in the mixed film between molecules.

The higher values of  $b_{1,12}$  occur when the content of POPC is low, being higher than the value of  $b_1$  of pure POPC, except for  $X_{\text{POPC}} = 0.394$ . This fact can be attributed to POPC breaking the compactness of DPPC, which results in an increase of the  $b_1$  coefficient (much more repulsion in respect to pure components). As has been seen previously, when  $X_{\text{POPC}} = 0.394$ , the excess area is negative, which is in agreement with the fact seen now that the  $b_{1,12}$  is the lowest value for the mixed films, and lower than that of pure POPC. Thus, the mixed film with  $X_{\text{POPC}} = 0.394$  is the most favourable among them.

Introducing the values of virial coefficients in Equations (6)–(9) and (10)–(13), values of  $G^E$  and  $\Delta G_{\text{mix}}$  have been calculated and reported in Table 6. It is seen that values of  $G^E$  are slightly positive, except for  $X_{\text{POPC}} = 0.394$  at low surfaces pressures; the values of  $\Delta G_{\text{mix}}$  are slightly negative. These values are in agreement with the previous comments about the mixing of the components in the film, that is, the interaction between components is not favoured but the entropic factor (see Equation (9)) leads to energetically favourable mixing. The mixing is especially favoured for  $X_{\text{POPC}} = 0.394$ , including the case of 35 mN/m of surface pressure which is close to the lateral pressure of biological membranes. Nevertheless, the positive values of  $G^E$  at 35 mN/m could indicate a propensity for phase separation, as is discussed in reference [45].

**Table 6.** Values of excess free energy and mixing energy at different compositions and surface pressures for POPC-DPPC mixed films.

$\pi$ (mN/m)	$X_{\text{POPC}}$	0.798	0.596	0.394	0.191
5	$G^E$ (J/mol)	202	211	−53	−6
	$\Delta G_{\text{mix}}$ (J/mol)	−1032	−1444	−1698	−1202
15	$G^E$ (J/mol)	538	667	56	318
	$\Delta G_{\text{mix}}$ (J/mol)	−696	−988	−1588	−878
25	$G^E$ (J/mol)	817	980	106	556
	$\Delta G_{\text{mix}}$ (J/mol)	−417	−675	−1539	−640
35	$G^E$ (J/mol)	1061	1144	48	645
	$\Delta G_{\text{mix}}$ (J/mol)	−174	−510	−1597	−551

### 3.3. Discussion

Isotherms indicate that a certain miscibility between components can be present in both cases: SA-OA and DPPC-POPC mixed films. The area vs. molar fraction ( $A$  vs.  $X$ ) analysis shows this effect of miscibility, but with less favourable interactions in respect to the individual components. Thus, the miscibility should be attributed to entropic factors. The less favourable interactions could be due, at least in part, to the presence of unsaturation in the hydrocarbon chains. The effect of unsaturations has also been discussed in reference [53] for the case of mixed films of a fatty acid and a phospholipid. The less favourable interactions lead to the partial phase segregation that is observed for the SA-OA system at high pressures and/or at high SA content. For the DPPC-POPC system, there is a composition ( $X_{\text{POPC}} \approx 0.4$ ) where the mixed film is more energetically favourable. A notable difference between both systems is that while the OA-SA system at  $X_{\text{OA}} \approx 0.4$  presents less favourable interactions, those of the POPC-DPPC system at  $X_{\text{POPC}} \approx 0.4$  are more favourable.

The values of the elastic modulus are more similar to those of the more fluid component (OA or POPC). The behaviour of the elastic modulus plot at high surface pressures is different, comparing both systems. The DPPC-POPC system presents only one maximum, meanwhile the OA-SA system presents two maxima with a clear phase in SA for the second maximum.

The analysis of the virial coefficients is similar in both systems, with the  $b_1$  values between those of the individual components. When comparing the  $b_1$  values for the fatty acids OA, SA and their mixed films with the  $b_1$  values for the phospholipids POPC, DPPC and their mixed films, lower values are observed, which indicates that these fatty acids can compact more easily than phospholipids. However, when analysing the excess values of  $b_1^E$  the differences are less significant, and give rise to the results derived from the area and energy analysis.

Ocko and Kelley [33] studied mixed monolayers of saturated stearic acid and of monounsaturated elaidic acid (the trans isomer of the oleic acid), and also observed poor miscibility with phase separation. Seoane et al. [34] reported mixed films of cholesterol with saturated or unsaturated fatty acids, but these are not discussed here due to the peculiar characteristics of cholesterol. Several authors [23,25–27,30,32] have also observed phase separation in fatty acid mixed monolayers of fluorinated and hydrogenated amphiphiles.

Comparing the behaviour of the POPC-DPPC mixed films with that of the unsaturated phospholipids POPC-POPE [35], it is shown that POPC-POPE mixed films demonstrate favourable mixing at all compositions, with negative values of the excess area,  $A^E$ , and with more negative values of the mixing energy,  $\Delta G_{\text{mix}}$ . Comparing the values of the virial coefficient  $b_1$  for DPPC, POPC and POPE [35], it was observed that DPPC presents the lowest value. As  $b_1$  is related to exclusion volumes and interactions between molecules, this means that the presence of a double bond provides higher exclusion volumes and more repulsive interactions between molecules. In contrast, the excess values  $b_1^E$  are always negative for the POPC-POPE mixed films [35] but positives for the POPC-DPPC ones (present work). This is in agreement with the obtained values of  $G^E$  which are positive for the POPC-DPPC mixed films, but negative for the POPC-POPE ones. Thus, mixed films of a saturated and

an unsaturated phospholipid seems to be energetically less favourable than those of two unsaturated phospholipids, at least from the cited systems that do not present enormous differences. On the other hand, Domenech et al. [36] suggest that cardiolipin and POPE can form separated phases under certain conditions, and that cardiolipin might be laterally segregated from POPE, even though thermodynamic analysis indicates miscibility.

Wydro and Witkowska [44] studied mixed films of phospholipids with different chains and unsaturations, through the mixtures of DPPG with DPPE, DSPE and DOPE. The results proved non ideal behaviour, as in the present case, and that the presence of the double bond in DOPE hamper the mixing and the layer compactness. The behaviour is also influenced by the type and length of the acyl chain. The values of  $G^E$  for DPPG-DOPE mixtures are positive (as in the present case) compared to the negative values of  $G^E$  for DPPG-DPPE and DPPG-DSPE mixed films, in which they exhibit saturated chains. The values of  $\Delta G_{mix}$  for DPPG-DOPE are negative (as in the present case) but less negative than those for DPPG-DPPE and DPPG-DSPE. Thus, as in the present case of the mixed films of POPC-DPPC, those of DPPG-DOPE present mixing due to the entropic factor. Dynarowicz et al. [37] studied miscibility and phase separation in mixed PC monolayers and found miscibility at low surface pressures but phase separation at high surface pressures.

Thus, phase separation is usual in mixed lipid monolayers due to differences in length, chemical groups or unsaturations in the acyl chain, differences in the headgroup, or the composition and surface pressure conditions.

#### 4. Conclusions

The presence of an unsaturation in the aliphatic chain of a fatty acid, e.g., oleic acid, or a phospholipid, e.g., POPC, in a mixed film with a saturated one, e.g., stearic acid or DPPC, respectively, makes molecular interaction less favourable, and causes the excess free energy to take positive values. Nevertheless, the entropic factor leads to slightly negative values in the mixing free energy. This situation facilitates phase separation (even partial mixing remains), especially with high contents of the saturated lipid and high surface pressures, since the saturated lipid tends to a more compact state. For the OA-SA mixed films, the most favourable mixing situation occurs at  $X_{OA} \approx 0.6$ ; meanwhile, for the POPC-DPPC it occurs at  $X_{POPC} \approx 0.4$ . The second virial coefficient  $b_1$  for the mixed films takes values between those of the individual components, but above those of an ideal mixing. The analysis of the mixed films with the virial state equation yields information on the molecular interactions, and permits us to easily calculate thermodynamic parameters. The elastic modulus behaviour for the mixed films exhibits closer values to the corresponding ones for the unsaturated component. For the POPC-DPPC mixed films, these are always in the LE state, similarly to POPC; meanwhile, for OA-SA mixed films, the LC state forms at high SA content and high surface pressures, probably due to the phase separation induced by SA.

**Funding:** This research received no external funding.

**Conflicts of Interest:** The authors declare no conflict of interest.

#### References

1. Ulman, A. *An Introduction to Ultrathin Organic Films*; Academic Press: Boston, MA, USA, 1990.
2. Petty, M.C. *Langmuir-Blodgett Films, An Introduction*; Cambridge University Press: Cambridge, MA, USA, 1996.
3. Richardson, T.H. (Ed.) *Functional Organic and Polymeric Materials: Molecular Functionality—Macroscopic Reality*; Wiley: Chichester, UK, 2000.
4. Baba, T.; Takai, K.; Takagi, T.; Kanamori, T. Effect of perfluoroalkyl chain length on monolayer behavior of partially fluorinated oleic acid molecules at the air–water interface. *Chem. Phys. Lipids* **2013**, *172*, 31–39. [[CrossRef](#)] [[PubMed](#)]

5. Barzyk, W.; Vuorinen, J. Application of the vibrating plate technique to measuring electric surface potential,  $\Delta V$ , of solutions; the flow cell for simultaneous measurement of the  $\Delta V$  and the surface pressure. *Colloids Surf. A* **2011**, *385*, 1–10. [[CrossRef](#)]
6. Dhathathreyan, A. Dissociation constants of long-chain hydroxy fatty acids in Langmuir-Blodgett films. *Colloids Surf. A* **2008**, *318*, 307–314. [[CrossRef](#)]
7. Dupres, V.; Cantin, S.; Benhabib, F.; Perrot, F.; Fontaine, P.; Goldmann, M.; Daillant, J.; Kononov, O. Superlattice formation in fatty acid monolayers on a divalent ion subphase: Role of chain length, temperature, and subphase concentration. *Langmuir* **2003**, *19*, 10808–10815. [[CrossRef](#)]
8. Kundu, S.; Raychaudhuri, A.K. Effect of water and air-water interface on the structural modification of Ni-arachidate Langmuir-Blodgett films. *J. Colloid Interf. Sci.* **2011**, *353*, 316–321. [[CrossRef](#)] [[PubMed](#)]
9. Mildner, J.; Dynarowicz-Latka, P.  $\beta$ -Carotene does not form a true Langmuir monolayer at the air-water interface. *Colloids Surf. B* **2012**, *90*, 244–247. [[CrossRef](#)] [[PubMed](#)]
10. Maheshwari, R.; Dhathathreyan, A. Influence of ammonium nitrate in phase transitions of Langmuir and Langmuir-Blodgett films at air/solution and solid/solution interfaces. *J. Colloid Interface Sci.* **2004**, *275*, 270–276. [[CrossRef](#)] [[PubMed](#)]
11. Snow, A.W.; Jernigan, G.G.; Ancona, M.G. Equilibrium spreading pressure and Langmuir-Blodgett film formation of omega-substituted palmitic acids. *Thin Solid Films* **2014**, *556*, 475–484. [[CrossRef](#)]
12. Yang, G.; Jiang, X.; Dai, S.; Cheng, G.; Zhang, X.; Du, Z. Morphology, Defect evolutions and nano-mechanical anisotropy of behenic acid monolayer. *Thin Solid Films* **2010**, *518*, 7086–7092. [[CrossRef](#)]
13. Ortiz-Collazos, S.; Gonçalves, Y.M.H.; Horta, B.A.C.; Picciani, P.H.S.; Louro, S.R.W.; Oliveira, O.N., Jr.; Pimentel, A.S. Langmuir films and mechanical properties of polyethyleneglycol fatty acids esters at the air-water interface. *Colloids Surf. A* **2016**, *498*, 50–57. [[CrossRef](#)]
14. Pantoja-Romero, W.S.; Estrada-López, E.D.; Picciani, P.H.S.; Oliveira, O.N., Jr.; Lachter, E.R.; Pimentel, A.S. Efficient molecular packing of glycerol monostearate in Langmuir monolayers at the air-water interface. *Colloids Surf. A* **2016**, *508*, 85–92. [[CrossRef](#)]
15. Rodríguez, J.F.F.; Dynarowicz-Latka, P.; Miñones-Conde, J. Structure of unsaturated fatty acids in 2D system. *Colloids Surf. B* **2017**, *158*, 634–642. [[CrossRef](#)] [[PubMed](#)]
16. Lunkenheimer, K.; Geggel, K.; Prescher, D. Role of counterion in the adsorption behavior of 1:1 ionic surfactants at fluid interfaces-Adsorption properties of alkali perfluoro-n-octanoates at the air/water interface. *Langmuir* **2017**, *33*, 10216–10224. [[CrossRef](#)] [[PubMed](#)]
17. Baba, T.; Takai, K.; Takagi, T.; Kanamori, T. Effect of the fluorination degree of hydrophobic chains on the monolayer behavior of unsaturated diacylphosphatidylcholines bearing partially fluorinated 9-octadecynoyl (stearoloyl) groups at the air-water interface. *Colloids Surf. B* **2014**, *123*, 246–253. [[CrossRef](#)] [[PubMed](#)]
18. Flasiński, M.; Wydro, P.; Broniatowski, M. Lyso-phosphatidylcholines in Langmuir monolayers-Influence of chain length on physicochemical characteristics of single-chained lipids. *J. Colloid Interface Sci.* **2014**, *418*, 20–30. [[CrossRef](#)] [[PubMed](#)]
19. Kaviratna, A.S.; Banerjee, R. The effect of acids on dipalmitoyl phosphatidylcholine (DPPC) monolayers and liposomes. *Colloids Surf. A* **2009**, *345*, 155–162. [[CrossRef](#)]
20. Rodríguez Niño, M.R.; Lucero, A.; Rodríguez Patino, J.M. Relaxation phenomena in phospholipid monolayers at the air-water interface. *Colloids Surf. A* **2008**, *320*, 260–270. [[CrossRef](#)]
21. Weis, M.; Ou-Yang, W.; Aida, T.; Yamamoto, T.; Manaka, T.; Iwamoto, M. Study of electrostatic energy contribution on monolayer domains size. *Thin Solid Films* **2008**, *517*, 1317–1320. [[CrossRef](#)]
22. Adams, E.M.; Casper, C.B.; Allen, H.C. Effect of cation enrichment on DPPC monolayers at the air-water interface. *J. Colloid Interface Sci.* **2016**, *478*, 353–364. [[CrossRef](#)] [[PubMed](#)]
23. Broniatowski, M.; Dynarowicz-Latka, P. Semifluorinated chains at the air/water interface: Studies of the interaction of a semifluorinated alkane with fluorinated alcohols in mixed Langmuir monolayers. *Langmuir* **2006**, *22*, 2691–2696. [[CrossRef](#)] [[PubMed](#)]
24. Brzozowska, A.M.; Mugele, F.; Duits, M.H.G. Stability and interactions in mixed monolayers of fatty acid derivatives on Artificial Sea Water. *Colloids Surf. A* **2013**, *433*, 200–211. [[CrossRef](#)]
25. Eftaiha, A.F.; Paige, M.F. Phase-separation of mixed surfactant monolayers: A comparison of film morphology at the solid-air and liquid-air interfaces. *J. Colloid Interface Sci.* **2012**, *380*, 105–112. [[CrossRef](#)] [[PubMed](#)]
26. Imae, T.; Takeshita, T.; Kato, M. Phase separation in hybrid Langmuir-Blodgett films of perfluorinated and hydrogenated amphiphiles. Examination by AFM. *Langmuir* **2000**, *16*, 612–621. [[CrossRef](#)]

27. Matsumoto, M.; Tanaka, K.; Azumi, R.; Kondo, Y.; Yoshino, N. Structure of phase-separated LB films of hydrogenated and perfluorinated carboxylic acids investigated by IR spectroscopy, AFM and FFM. *Langmuir* **2003**, *19*, 2802–2807. [[CrossRef](#)]
28. Matsumoto, M.; Tanaka, K.; Azumi, R.; Kondo, Y.; Yoshino, N. Template-directed patterning using phase-separated LB films. *Langmuir* **2004**, *20*, 8728–8734. [[CrossRef](#)] [[PubMed](#)]
29. Qaqish, S.E.; Paige, M.F. Characterization of domain growth kinetics in a mixed perfluorocarbon-hydrocarbon Langmuir-Blodgett monolayer. *J. Colloid Interface Sci.* **2008**, *325*, 290–293. [[CrossRef](#)] [[PubMed](#)]
30. Watanabe, S.; Okuda, R.; Azumi, R.; Sakai, H.; Abe, M. Effect of subphase temperature on the phase-separated structures of mixed Langmuir and Langmuir-Blodgett films of fatty acids and hybrid carboxylic acids. *J. Colloid Interface Sci.* **2011**, *363*, 379–385. [[CrossRef](#)] [[PubMed](#)]
31. Rehman, J.; Sowah-Kuma, D.; Stevens, A.L.; Bu, W.; Paige, M.F. Mixing behaviour in binary anionic gemini surfactant-perfluorinated fatty acid Langmuir monolayers. *Langmuir* **2017**, *33*, 10205–10215. [[CrossRef](#)] [[PubMed](#)]
32. Paige, M.F.; Eftaiha, A.F. Phase-separated surfactant monolayers: Exploiting immiscibility of fluorocarbons and hydrocarbons to pattern interfaces. *Adv. Colloid Interface Sci.* **2017**, *248*, 129–146. [[CrossRef](#)] [[PubMed](#)]
33. Ocko, B.M.; Kelley, M.S.; Nikova, A.T.; Schwartz, D.K. Structure and Phase Behavior of Mixed Monolayers of Saturated and Unsaturated Fatty Acids. *Langmuir* **2002**, *18*, 9810–9815. [[CrossRef](#)]
34. Seoane, R.; Dynarowicz-Latka, P.; Miñones, J., Jr.; Rey, I. Mixed Langmuir monolayers of cholesterol and essential fatty acids. *Colloid Polym. Sci.* **2001**, *279*, 562–570. [[CrossRef](#)]
35. Domenech, O.; Torrent-Burgués, J.; Merino, S.; Sanz, F.; Montero, M.T.; Hernández-Borrell, J. Surface thermodynamics study of monolayers formed with heteroacid phospholipids of biological interest. *Colloids Surf. B* **2005**, *41*, 233–238. [[CrossRef](#)] [[PubMed](#)]
36. Domènech, O.; Sanz, F.; Montero, M.T.; Hernández-Borrell, J. Thermodynamic and structural study of the main phospholipid components comprising the mitochondrial inner membrane. *Biochim. Biophys. Acta* **2006**, *1758*, 213–221. [[CrossRef](#)] [[PubMed](#)]
37. Dynarowicz-Latka, P.; Wnetrzak, A.; Broniatowski, M.; Flasiński, M. Miscibility and phase separation in mixed erucylphosphocholine-DPPC Monolayers. *Colloids Surf. B* **2013**, *107*, 43–52. [[CrossRef](#)] [[PubMed](#)]
38. Garcia-Manyes, S.; Domènech, O.; Sanz, F.; Montero, M.T.; Hernandez-Borrell, J. Atomic force microscopy and force spectroscopy study of Langmuir-Blodgett films formed by heteroacid phospholipids of biological interest. *Biochim. Biophys. Acta* **2007**, *1768*, 1190–1198. [[CrossRef](#)] [[PubMed](#)]
39. Ohki, S.; Müller, M.; Arnold, K.; Ohshima, H. Surface potential of phosphoinositide membranes: Comparison between theory and experiment. *Colloids Surf. B* **2010**, *79*, 210–218. [[CrossRef](#)] [[PubMed](#)]
40. Park, J.-W. Individual leaflet phase effect on nanometer-scale surface properties of phospholipid bilayers. *Colloids Surf. B* **2009**, *71*, 128–132. [[CrossRef](#)] [[PubMed](#)]
41. Stefaniu, C.; Brezesinski, G. Grazing incidence X-ray diffraction studies of condensed double-chain phospholipid monolayers formed at the soft air/water interface. *Adv. Colloid Interface Sci.* **2014**, *207*, 265–279. [[CrossRef](#)] [[PubMed](#)]
42. Wydro, P. The influence of cardiolipin on phosphatidylglycerol/ phosphatidylethanolamine monolayers—Studies on ternary films imitating bacterial membranes. *Colloids Surf. B* **2013**, *106*, 217–223. [[CrossRef](#)] [[PubMed](#)]
43. Wydro, P. The influence of cholesterol on multicomponent Langmuir monolayers imitating outer and inner leaflet of human erythrocyte membrane. *Colloids Surf. B* **2013**, *103*, 67–74. [[CrossRef](#)] [[PubMed](#)]
44. Wydro, P.; Witkowska, K. The interactions between phosphatidylglycerol and phosphatidylethanolamines in model bacterial membranes. The effect of the acyl chain length and saturation. *Colloids Surf. B* **2009**, *72*, 32–39. [[CrossRef](#)] [[PubMed](#)]
45. Olżyńska, A.; Zubek, M.; Roeselova, M.; Korchowicz, J.; Cwiklik, L. Mixed DPPC/POPC monolayers: All-atom molecular dynamics simulations and Langmuir monolayer experiments. *Biochim. Biophys. Acta* **2016**, *1858*, 3120–3130. [[CrossRef](#)] [[PubMed](#)]
46. Hoyo, J.; Torrent-Burgués, J.; Gaus, E. Biomimetic monolayer films of monogalactosyldiacylglycerol incorporating ubiquinone. *J. Colloid Interface Sci.* **2012**, *384*, 189–197. [[CrossRef](#)] [[PubMed](#)]
47. Vitovič, P.; Nikolelis, D.P.; Hianik, T. Study of calix [4] resorcinarene–dopamine com-plexation in mixed phospholipid monolayers formed at the air | water interface. *Biochim. Biophys. Acta* **2006**, *1758*, 1852–1861. [[CrossRef](#)] [[PubMed](#)]

48. Hoyo, J.; Gaus, E.; Torrent-Burgués, J. Monogalactosyldiacylglycerol and digalactosyldiacylglycerol role, physical states, applications and biomimetic monolayer films. *Eur. Phys. J. E* **2016**, *39*, 39. [[CrossRef](#)] [[PubMed](#)]
49. Hoyo, J.; Gaus, E.; Torrent-Burgués, J. Tuning ubiquinone position in biomimetic monolayer membranes. *Eur. Phys. J. E* **2017**, *40*, 62. [[CrossRef](#)] [[PubMed](#)]
50. Birdi, K.S.; Gevod, V.S. Melittin and ionic surfactant interactions in monomolecular films. *Colloid Polym. Sci.* **1987**, *265*, 257–261. [[CrossRef](#)]
51. Davies, J.T.; Rideal, E.K. *Interfacial Phenomena*; Academic Press: Cambridge, MA, USA, 1993.
52. Avantilipids. Available online: <https://avantilipids.com/tech-support/physical-properties/> (accessed on 10 April 2018).
53. Nakata, S.; Seki, Y.; Nomura, M.; Fukuhara, K.; Denda, M. Characteristic Isotherms for a Mixed Molecular Layer Composed of Phospholipid and Fatty Acid. *Bull. Chem. Soc. Jpn.* **2017**, *90*, 801–806. [[CrossRef](#)]



© 2018 by the author. Licensee MDPI, Basel, Switzerland. This article is an open access article distributed under the terms and conditions of the Creative Commons Attribution (CC BY) license (<http://creativecommons.org/licenses/by/4.0/>).